

GOREL Lukáš, VITTEK Ján, SZYCHTA Elżbieta

## COMPARISON OF VECTOR CONTROL METHODS FOR ELIMINATION OF TORSIONAL VIBRATIONS IN AC DRIVES

### Abstract

The paper compares three vector control strategies for elimination of torsion vibrations. The first algorithm is based on classical IPD controller of the system with flexible coupling described in state space. The second algorithm is based on force dynamics control and the third one exploits sliding mode control. All three algorithms respect vector control of synchronous motor with permanent magnets. Matlab-Simulink environment is used to evaluate performance of all three control algorithms.

### 1. INTRODUCTION

Mechanical coupling between motor shaft and load is composed of materials with some degree of elasticity. This elasticity combined with inertia causes oscillation of the mechanical coupling which results in undesirable effect on drive's control performance.

### 2. MOTOR MODEL CONSIDERING MECHANICAL COUPLING WITH TORSION OSCILLATIONS

For simulations standard model of synchronous motor with permanent magnets (SMPM) is used. To ensure comparable conditions, similar to practical applications all three simulations contains three-phase voltage converter for SMPM control. To analyze control system performances mathematical model of SMPM and flexible coupling is developed. Equations (1), (2) and (3) describe SMPM.

$$\frac{di_d}{dt} = \frac{1}{L_d}(u_d - R_s i_d + p\omega_R \Psi_q) \quad \frac{di_q}{dt} = \frac{1}{L_q}(u_q - R_s i_q - p\omega_R \Psi_d) \quad (1)$$

$$\Psi_d = L_d i_d + \Psi_{PM} \quad \Psi_q = L_q i_q \quad (2)$$

$$\frac{d\omega_R}{dt} = \frac{1}{J_R}(M_{el} - M_{Ls}) \quad M_{el} = \frac{3}{2} p (\Psi_d i_q - \Psi_q i_d) \quad (3)$$

Block diagram of mechanical coupling, which is shown in **Fig.1** is described by equations (5), (6) and (7). Simplified model of flexible coupling doesn't respects damping coefficient, which makes situation for control algorithms even worse due to fact that torsional oscillations are keeping their maximum value. The blue blocks of **Fig.1** introduce load side. The brown blocks correspond to motor side mechanical parts. Transfer function of mechanical coupling

is derived directly from **Fig.1** using Mason's formula and results in (6). For shaft with circular cross section flexible coupling coefficient,  $K_s$  can be calculated as (4).

$$K_s = \frac{\pi D^4 G}{32l}, \quad (4)$$

where  $D$  is diameter of shaft,  $G$  is modulus of elasticity and  $l$  is shaft length.

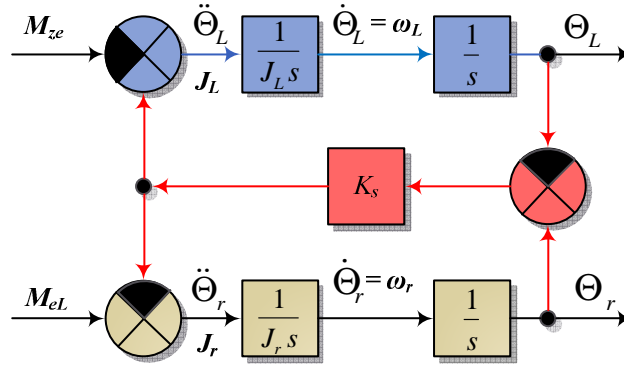


**Fig. 1** Equivalent block diagram of flexible coupling between motor and load

$$\frac{d\theta_R}{dt} = \omega_R, \quad \frac{d\omega_R}{dt} = \frac{1}{J_R} (M_{el} - M_{Ls}) \quad (5)$$

$$\frac{d\theta_L}{dt} = \omega_L, \quad \frac{d\omega_L}{dt} = \frac{1}{J_L} (M_{Ls} - M_{Le}) \quad (6)$$

$$F(s) = \frac{\theta_R}{M_{el}} = \frac{s^2 + \omega_a^2}{s^2 J_R (s^2 + \omega_r^2)}, \quad \omega_r = \sqrt{\frac{K_s}{J_R} + \frac{K_s}{J_L}}, \quad \omega_a = \sqrt{\frac{K_s}{J_L}}, \quad (7)$$

where  $\theta$  is position, index  $r$  is for rotor and  $L$  is index for load respectively.  $\omega$  is speed in rad/s with the same indexing,  $J$  is motor and load moment of inertia.  $M_{eL}$  is electromagnetic torque and  $M_{Ls}$  is torque generated by different value between rotor and load position. This torque is proportional to the position displacement and can be expressed as :

$$M_{Ls} = K_s (\theta_R - \theta_L) + K_t (\omega_R - \omega_L) \quad (8)$$

This is valid if coefficient  $K_t$  is considered. Further damping and friction are neglected in simulations. Spring torque,  $M_{Ls}$  is calculated as :

$$M_{Ls} = K_s (\theta_R - \theta_L) \quad (9)$$

### 3. TORSIONAL VIBRATIONS MINIMALIZATION ALGORITHMS

#### I. IPD regulator in state space for elimination of vibration

The first method exploits control in state-space [1]. In this case, analogy of IPD regulator can be used. Since this is a state-space control system of the fourth order (see **Fig.2**) feedbacks of four state variables are required. To minimize number of sensors derivatives for speed are computed mathematically.

Gains of feedback loops are adjusted to ensure the prescribed settling time. Feedback gain values are determined using the pole placement method. Transfer function of block diagram shown as **Fig. 2** is obtained by Mason's formula is fifth order.

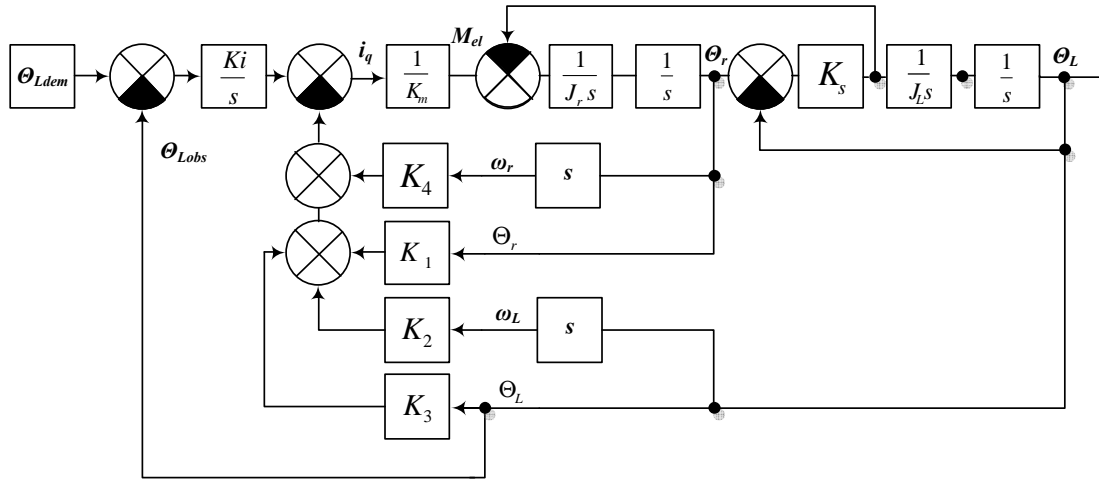


**Fig. 2** Block diagram for load angle control system with IPD regulators

$$\frac{\theta_L(s)}{\theta_{Ldem}(s)} = \frac{1}{\frac{K_m J_r J_L}{K_i K_s} s^5 + \frac{K_4 J_L}{K_i K_s} s^4 + \frac{K_m K_s (J_r + J_L) + K_1 J_L}{K_i K_s} s^3 + \frac{K_4 + K_2}{K_i} s^2 + \frac{K_1 + K_3}{K_i} s + 1} \quad (10)$$

At first the ideal transfer function for the system of fifth order can be calculated by Dodd's formula, (11) where  $n$  is the system order (in this case  $n = 5$ ). Comparison of the same degree coefficients in (10) and (11) gives parameters of  $K_{1,2,3,4}$  and  $K_i$ .

$$\frac{\theta_L(s)}{\theta_{Ldem}(s)} = \left[ \frac{1}{\frac{T_{s\theta L}}{1,5(1+n)} s + 1} \right]^n \quad (11)$$

$$K_i = \frac{K_m J_r J_L}{K_s} \left( \frac{9}{T_{s\theta L}} \right)^5 \quad K_4 = K_m J_r 5 \left( \frac{9}{T_{s\theta L}} \right) \quad (12)$$

$$K_1 = K_m J_r 10 \left( \frac{9}{T_{s\theta L}} \right)^2 - K_m K_s \left( 1 + \frac{J_r}{J_L} \right)^2 \quad (13)$$

$$K_2 = \frac{K_m J_r J_L}{K_s} 10 \left( \frac{9}{T_{s\theta L}} \right)^3 - K_4 \quad K_3 = \frac{K_m J_r J_L}{K_s} 5 \left( \frac{9}{T_{s\theta L}} \right)^4 - K_1 \quad (14)$$

This system requires information about load angle, which is its disadvantage. Therefore observer is designed to calculate load side parameters from rotor position and torque component of stator current,  $i_q$ . Observer of load state variables is based on real time model of two mass system [2]. System state equations are :

$$\begin{aligned} s\theta_L &= \omega_L; & s\theta_r &= \omega_r; \\ s\omega_L &= \frac{1}{J_L} [K_s(\theta_r - \theta_L) - M_{Le}]; & s\omega_r &= \frac{1}{J_r} [M_{eL} - K_s(\theta_r - \theta_L)] \\ -sM_{Le} &= 0 \end{aligned} \quad (15)$$

Matrix form of observer is defined as:

$$\begin{bmatrix} \hat{\theta}_L \\ \hat{\theta}_r \\ \hat{\omega}_r \\ \hat{\omega}_L \\ -\hat{M}_{Le} \end{bmatrix} = \begin{bmatrix} 0 & 0 & 1 & 0 & 0 \\ 0 & 0 & 0 & 1 & 0 \\ -a_1 & a_1 & 0 & 0 & -a_2 \\ a_3 & -a_3 & 0 & 0 & 0 \\ 0 & 0 & 0 & 0 & 0 \end{bmatrix} \begin{bmatrix} \hat{\theta}_L \\ \hat{\theta}_r \\ \hat{\omega}_r \\ \hat{\omega}_L \\ -\hat{M}_{Le} \end{bmatrix} + \begin{bmatrix} 0 \\ 0 \\ 0 \\ a_4 \\ 0 \end{bmatrix} M_{el} + \begin{bmatrix} k_{\theta 1} \\ k_{\theta 2} \\ k_{\omega 1} \\ k_{\omega 1} \\ k_{M1} \end{bmatrix} (\theta_r - \hat{\theta}_r), \quad (16)$$

Subtracting observer equations from equations of the system forms dynamical error system with coefficients defined as:

$$a_1 = \frac{K_s}{J_L}; \quad a_2 = \frac{1}{J_L}; \quad a_3 = \frac{K_s}{J_r}; \quad a_4 = \frac{1}{J_r}; \quad (17)$$

Eigenvalues of the system matrix must have a negative real parts to ensure convergence of the state estimates toward real system variables. If pole-placement method with multiple poles placed in  $\omega=1/T_u$  is used then observer eigenvalues (18) can be determined by comparison with desired polynomial, (20) which results in:

$$\lambda^5 + \lambda^4 k_{\theta 2} + \lambda^3 (a_3 + a_1 + k_{\omega 2}) + \lambda^2 (a_3 k_{\theta 1} + a_1 k_{\theta 2}) + \lambda (a_1 k_{\omega 2} + a_3 k_{\omega 1}) + a_2 a_3 K_{M1} \quad (18)$$

$$T_{u2} = 1,5(1+n) \frac{1}{\omega_0} \Rightarrow \omega_0 = \frac{9}{T_{u2}} \quad (19)$$

$$(\lambda + \omega_0)^5 = \left( \lambda + \frac{9}{T_{u2}} \right)^5 = \lambda^5 + \lambda^4 \frac{45}{T_{u2}} + \lambda^3 \frac{810}{T_{u2}^2} + \lambda^2 \frac{7290}{T_{u2}^3} + \lambda \frac{32805}{T_{u2}^4} + \frac{59049}{T_{u2}^5} \quad (20)$$

Comparing the coefficients of the same degree (18) defines observer gains as:

$$\begin{aligned} k_{\theta L} &= \frac{J_L}{K_s} \left( \frac{7290 J_L - 45 K_s T_{u2}}{J_L T_{u2}^3} \right); & k_{\theta r} &= \frac{45}{T_{u2}}; \\ k_{\omega L} &= \frac{J_L}{K_s} \left( \frac{32805 J_L^2 J_r - 810 K_s J_L J_r T_{u2}^2 + K_s^2 J_L T_{u2}^4 + K_s^2 J_r T_{u2}^4}{J_L^2 J_r T_{u2}^4} \right); & & \\ k_{\omega r} &= \frac{810}{T_{u2}^2} - \frac{K_s}{J_L} - \frac{K_s}{J_r}; & k_{MLe} &= \frac{J_L J_r 59049}{K_s T_{u2}^5}; \end{aligned} \quad (21)$$

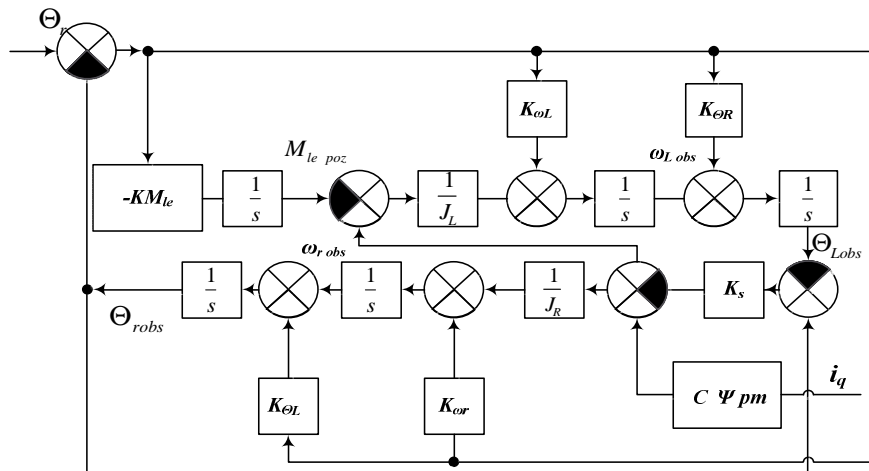


**Fig. 3.** Block diagram of load side variables observer

It is clear that observer based on rotor angle and stator current torque component measurement produces all necessary informations about load side state variables. Connection of these two models (*model of flexible coupling a model of state-space observer*) eliminates sensor on the load side.

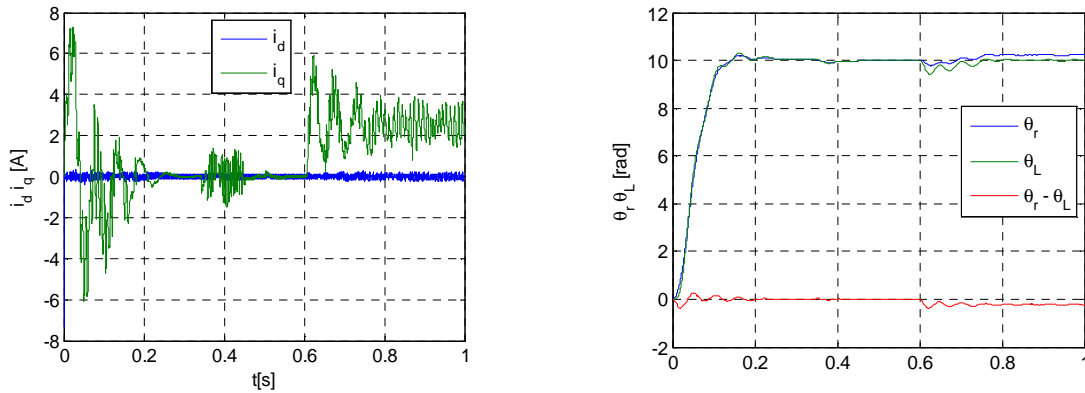


**Fig. 4** Currents, load and rotor position and difference between them IPD

## II. Elimination of vibrations using Forced Dynamics Control

Control system for elimination of torsional vibrations using FDC is more complex [2]. FDC control law is developed in two steps. Firstly feedback linearization principles are applied to inner speed control loop, which requires load torque estimate. Secondly the design of the position control loop is also based on FDC and estimated position and speed of load are used for control. Overall control system therefore contains three observers (*torque on the shaft of motor, load side mechanical variables and load side torque including its derivatives*).

All observers parameter are set up by using Dodd's settling time formula. State observer was described by (12), (13), (14), and shown in **Fig. 3**. The observer offers all state variables desired by FDC algorithm. FDC load position control law requires estimate of load torque and its first and second derivative. These derivatives of load torque are produced in separate observer based on Luenberger principles, which is described as:

$$\frac{dM_{Le}}{dt} = \dot{M}_{Le}; \quad \frac{d\dot{M}_{Le}}{dt} = \ddot{M}_{Le}; \quad \frac{d\ddot{M}_{Le}}{dt} = 0; \quad (22)$$

Observer's state equations rewritten in matrix form including determinant are defined as:

$$\begin{bmatrix} \hat{\dot{M}}_{Le} \\ \hat{\ddot{M}}_{Le} \\ \hat{\ddot{M}}_{Le} \end{bmatrix} = \begin{bmatrix} 0 & 1 & 0 \\ 0 & 0 & 1 \\ 0 & 0 & 0 \end{bmatrix} \begin{bmatrix} \hat{M}_{Le} \\ \hat{\dot{M}}_{Le} \\ \hat{\ddot{M}}_{Le} \end{bmatrix} + \begin{bmatrix} k_1 \\ k_2 \\ k_3 \end{bmatrix} (M_{Le} - \hat{M}_{Le}); \quad \det \begin{bmatrix} \lambda + k_1 & -1 & 0 \\ k_2 & \lambda & -1 \\ k_3 & 0 & \lambda \end{bmatrix} = \lambda^3 + \lambda^2 k_1 + \lambda k_2 + k_3 \quad (23)$$

Using Dodd's formula and comparing variables of the same order:

$$T_{u2} = 1,5(1+n) \frac{1}{\omega_0} \Rightarrow \omega_0 = \frac{6}{T_{u3}}; \quad (\lambda + \omega_0)^3 = \left( \lambda + \frac{9}{T_{u2}} \right)^3 = \lambda^3 + \lambda^2 \frac{18}{T_{u3}} + \lambda \frac{108}{T_{u3}^2} + \frac{216}{T_{u3}^3}, \quad (24)$$

results in observer gains:

$$k_1 = \frac{18}{T_{u3}}; \quad k_2 = \frac{108}{T_{u3}^2}; \quad k_3 = \frac{216}{T_{u3}^3}; \quad (25)$$

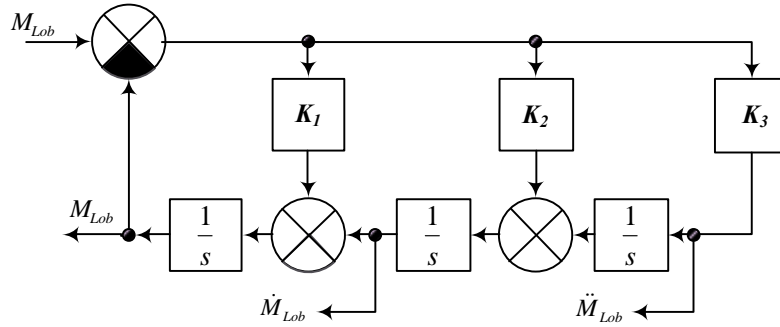


**Fig. 5** Load torque observer

Speed control loop based on FDC requires the estimate of torque on the shaft of motor as input. For this purpose the observer based on motor mechanical equations completed with differential equation for shaft torque, which is taken as state-variable, is developed as.

$$\frac{d\theta_r}{dt} = \omega_r; \quad \frac{d\omega_r}{dt} = \frac{1}{J_r} (c(\psi_d i_q - \psi_q i_d) - M_{Ls}); \quad -\frac{dM_{Ls}}{dt} = 0 \quad (26)$$

In matrix form system equations has form:

$$\begin{bmatrix} \dot{\theta}'_r \\ \dot{\omega}'_r \\ -\dot{M}'_{Ls} \end{bmatrix} = \begin{bmatrix} 0 & 1 & 0 \\ 0 & 0 & -a_4 \\ 0 & 0 & 0 \end{bmatrix} \begin{bmatrix} \theta'_r \\ \omega'_r \\ -M'_{Ls} \end{bmatrix} + \begin{bmatrix} 0 \\ c\Psi_{pm} i_g \\ 0 \end{bmatrix} + \begin{bmatrix} k_\theta \\ k_\omega \\ k_m \end{bmatrix} (\theta_r - \theta'_r) \quad (27)$$

Same approach described previously is used to define observer gains:

$$\det \begin{bmatrix} \lambda + k_\theta & -1 & 0 \\ k_\omega & \lambda & a_4 \\ -k_M & 0 & \lambda \end{bmatrix} = \lambda^3 + \lambda^2 k_\theta + \lambda k_\omega + k_M a_4 \quad (28)$$

$$T_{u2} = 1,5(1+n) \frac{1}{\omega_0} \Rightarrow \omega_0 = \frac{6}{T_{u1}}; \quad (\lambda + \omega_0)^3 = \left( \lambda + \frac{9}{T_{u1}} \right)^3 = \lambda^3 + \lambda^2 \frac{18}{T_{u1}} + \lambda \frac{108}{T_{u1}^2} + \frac{216}{T_{u1}^3} \quad (29)$$

$$k_\theta = \frac{18}{T_{u1}}; \quad k_\omega = \frac{108}{T_{u1}^2}; \quad k_M = \frac{216}{T_{u1}^3} J_r; \quad (30)$$

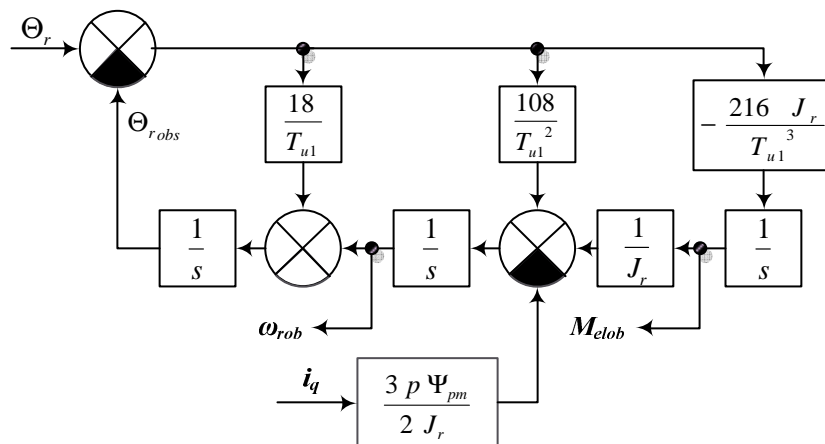


**Fig. 6** Motor load torque observer

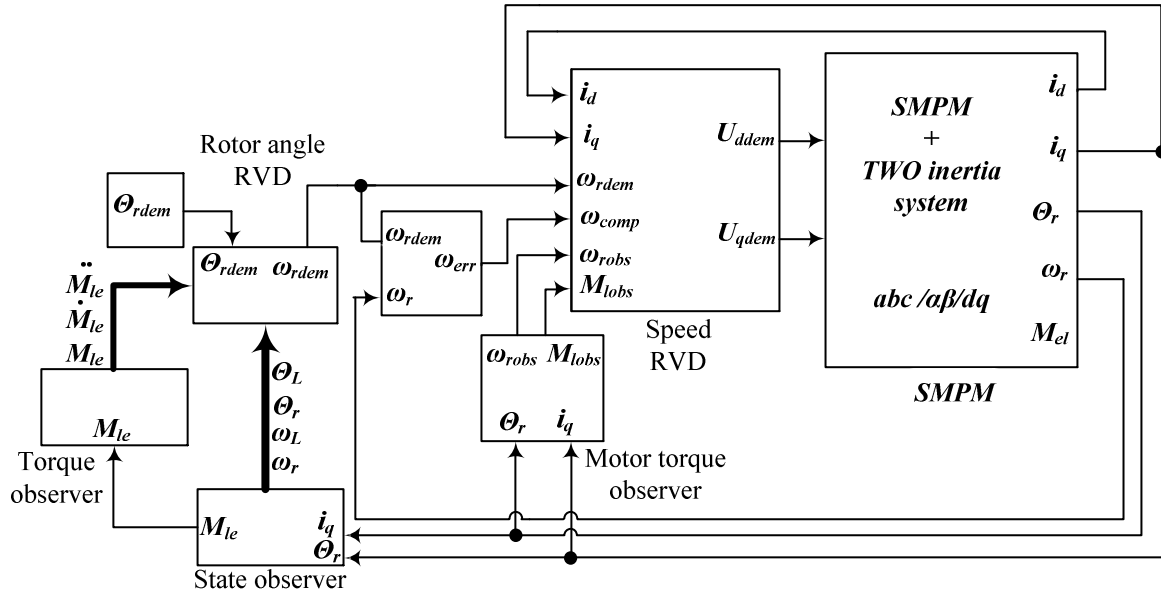


**Fig. 7** Position FDC diagram

Simulation results of load position control based on the principles of FDC are shown in **Fig. 8** and shows satisfactory elimination of torsional vibrations.

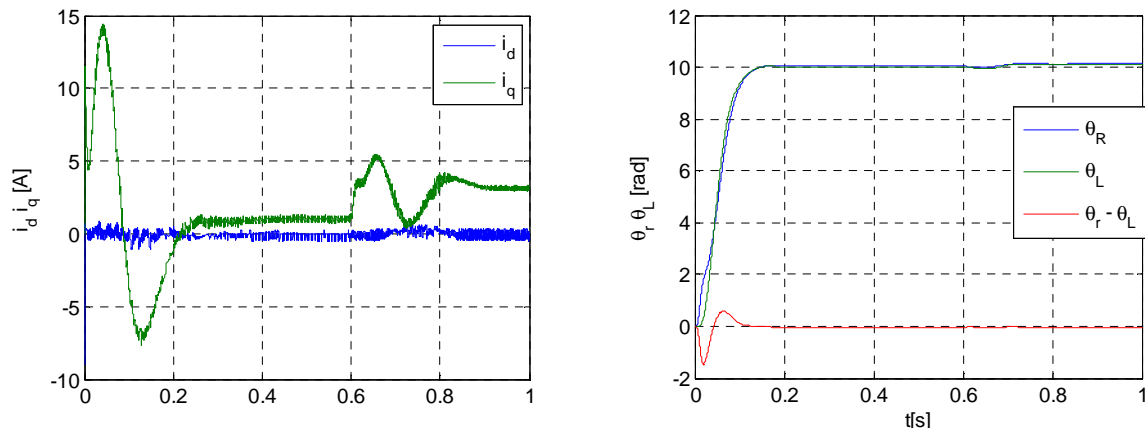


**Fig. 8** Currents, load and rotor position and difference between them FDC

### III. Elimination of vibrations using Sliding Mode Control

SMC is a form of control technique supporting state feedback in which control variable,  $u$  switches between two limits,  $\pm u_{\max}$  usually defined by voltage of DC bus. Switching function is defined as (32) where vector  $\mathbf{y}$  is given as shows (33). Rewritten linear differential equation for switching boundary has form (34) and is decisive for control system behaviour. Control variable switches between its to limits as define (35). For zero initial conditions the closed loop transfer function has form as defined (36).

$$u = -u_{\max} \text{sign}[S(\mathbf{y}, y_{dem})] \quad (31)$$

$$S(\mathbf{y}, y_{dem}) = y - y_{dem} + \sum_{i=1}^{r-1} w_i y^i \quad (32)$$

$$\mathbf{y} = [y \dot{y} \ddot{y} \dots y^{(r-1)}]^T \quad (33)$$

$$y_{dem}(s) = y(s) \left[ 1 + \sum_{i=1}^{r-1} w_i s^{(i)} \right] \quad (34)$$

$$S(y, y_{dem}) = 0 \quad (35)$$

$$\frac{y(s)}{y_{dem}(s)} = \frac{1}{1 + w_1 s + w_2 s^2 + \dots + w_n s^n} \quad (36)$$

More about step by step calculation of switching function can be found in [3].

$$\omega_{rdem} = K_{sm} \left[ \int (\theta_{Ldem} - \theta_L) dt - 4 \frac{2}{15} T_{sa} \theta_L - 6 \left( \frac{2}{15} T_{sa} \right)^2 \omega_L - 4 \left( \frac{2}{15} T_{sa} \right)^3 \varepsilon_L - \left( \frac{2}{15} T_{sa} \right)^4 \dot{\varepsilon}_L \right]$$

This is a final form of SMC algorithm, block diagram of which shows Fig. 9.

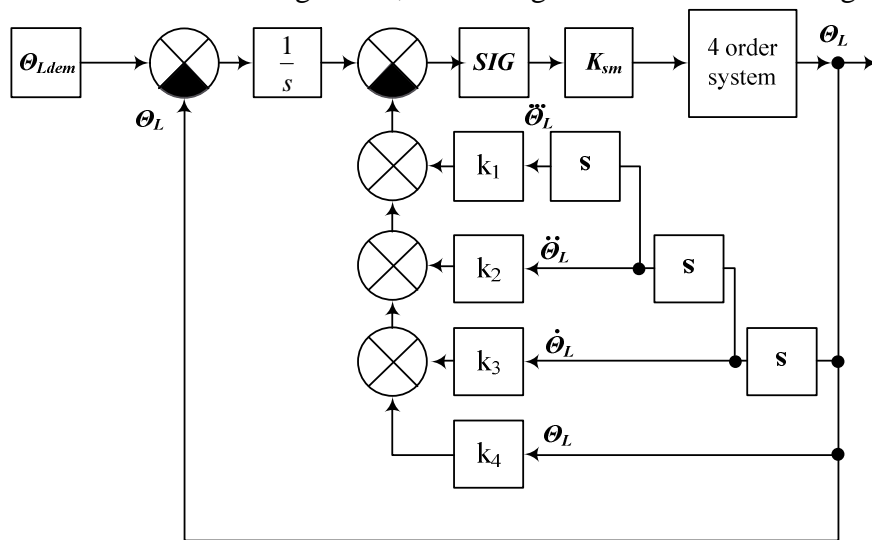


**Fig. 9** Block diagram of SMC

This is basic diagram of SMC for control of load position. If we can use single rotor position sensor observer must be added in to overall control structure. State space observer already presented was added to calculated load angle and load speed. Further derivation required was obtained by the regular derivation block. Block diagram of the SMC control system is shown in **Fig.9**.

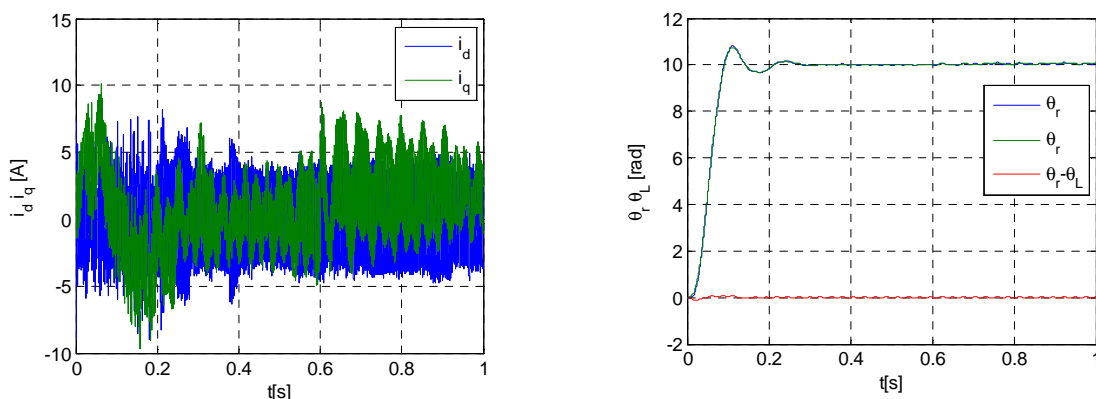


**Fig. 10** Currents, load and rotor position and difference between them SMC



## CONCLUSION

Comparison of simulation results presented confirmed that all three presented methods effectively eliminate torsional vibrations and necessary modifications of shaft diameter or its material [9] are avoided.

The most widely used method in practice is elimination of vibrations using PID controllers but as it was shown the other methods provide equally good or even better results. Detailed analysis of such controller results in an important observation that the different pole-assignment patterns is necessary for the different inertia ratios between load and motor [10].

FDC method has especially smooth stator current components and provides close tracking of prescribed dynamics. Disadvantage of FDC if compared to IPD is its computational complexity due to necessity of load torque derivatives estimation [11]. Taking into account that both methods used pole placement method to adjust control gains under the same conditions, simulations confirm that FDC eliminates torsion oscillations more effectively.

SMC is a robust control technique, which exploits switching of control variable between its two maximum values [12]. This is the reason why stator current has higher oscillations than in previously evaluated methods. If higher switching frequency of inverter is employed or higher quality observation is used the motor current ripples can be substantially reduced, which will result in near-equivalent control performance.

## ACKNOWLEDGEMENT

The authors wish to thank for support the Slovak Grant agency VEGA No. 1/0355/11.

## REFERENCES

1. J. VITTEK, S.J. DODDS: "Forced Dynamics Control of Electric Drives", EDIS University of Žilina, 2003, ISBN 80-8070-087-7.
2. J. VITTEK, P. BRIŠ, P. MAKYŠ, M. ŠTULRAJTER: "Forced Dynamics Control of PMSM Drives with Torsion Oscillations", COMPEL, Vol. 29, No. 1, 2010, ISBN 0332-1649.
3. R. MACKO, M. ŽALMAN: "New Methodology of the Design of Speed Controller for Servo-drive with Two-inertia Flexible System", AT&T Journal, 2/2006, pp.106-110, ISBN 80-227-2431-9.
4. J. VITTEK, P. BRIŠ, M. ŠTULRAJTER, P. MAKYŠ, V. COMNAC, M. CERNAT: "Chattering Free Sliding Mode Control Law for the Drive employing PMSM Position Control", OPTIM, 2008, ISBN: 978-1-4244-1544-1.
5. J. VITTEK, P. MAKYŠ: "Forced Dynamics Control – Advantages and Disadvantages", ATP Journal, 2/2011, 2011, 02, pp.: 14, ISSN: 1336-233X.
6. J. VITTEK, M. POSPÍŠIL, P. LEHOČKÝ: "Speed and Position Forced Dynamics Control of Servo-drives", Central European School of Doctoral Study in the Field of Power Electrical Engineering and Automation", Trenčianske Teplice, Slovakia, 20.-22. Sept. 2011, pp.: 120-127, ISBN 978-80-554-0421-9.
7. S. J. DODDS, J. VITTEK: "Sliding Mode Vector Control of PMSM Drives with Flexible Couplings in Motion Control", Proc. of the Advances in Computing and Technology AC&T conf. 2009, London, United Kingdom, 2009, 01, 27.-28, pp.: 77-85.
8. S. J. Dodds, J. Vittek, R. Perryman, J. Kuchta: "Sliding Mode Control of PMSM Electric Drives with Flexible Coupling", Proc. of EDPE '07 conf., 24-26 Sept. 2007, High Tatras, ISBN: 978-80-8073-868-6.
9. J. Moravec, Stroka, R.: "Magnetic Warm Forming" 13<sup>th</sup> International Research/Expert conf. "Trends in the Development of Machinery and Associated Technology", TMT 2009, Hammamet, Tunisia, 16.-21. Oct. 2009, pp.: 357-360, ISBN 1840-4944G.

10. G. Zhang, J. Furusho: "Speed Control of Two-inertia System by PI/PID Control", IEEE Trans. on Industrial Electronics, vol. 47, no. 3, 2000, pp. 603-609, ISSN 0278-0046.
11. J. Vittek, V. Vavrus, P. Bris, L. Gorel: "Forced Dynamics Control of the Elastic Joint Drive with Single Rotor Position Sensor", Automatika, vol. 54, 2013, pp.; 337-347, Croatia, ISSN: 1848-3380.
12. J. Vittek, S. Ryvkin: "Decomposed Sliding Mode Control of the Drive with IPMSM and Flexible Coupling", Mathematical Problems in Engineering, Vol. 2013, Variable Structure Systems and Applications, Hindawi Publishing Corporation, ISSN: 1563-5147, (*in printing*). <http://dx.doi.org/10.1155/2013/680376>.

***Authors:***

University of Žilina, Faculty of Electrical Engineering, Department of Power Electrical Systems, Veľký Diel, 01026 Žilina, SLOVAKIA, phone: +421 041 513 2155, email: Jan.Vittek@fel.uniza.sk

Kazimierz Pulaski University of Technology and Humanities in Radom, Faculty of Transport and Electrical Engineering, POLAND; Radom 26-600; Malczewskiego 29, phone: +48 48 361-77-00, email: e.szychta@uthrad.pl